PHYSICAL REVIEW B **78**, 081404(R) (2008)

Time-domain analysis of mechanism of plasmon-assisted extraordinary optical transmission

Yun-Song Zhou,[1,*] Ben-Yuan Gu,[2,†] Sheng Lan,[3] and Li-Ming Zhao[1]
[1]*Department of Physics, Capital Normal University, Beijing 100037, China*
[2]*Institute of Physics, Chinese Academy of Sciences, P.O. Box 603, Beijing 100080, China*
[3]*Laboratory of Photonic Information Technology, School for Information and Optoelectronic Science and Engineering, South China Normal University, Guangzhou, Guangdong 510006, China*
(Received 10 June 2008; published 22 August 2008)

We present the time-domain analysis of the extraordinary optical transmission of the slits milled on the thin metallic film. We employ the finite-difference time-domain method to study the variations of the transmission energies with the sampling time received by several monitors that are placed on the specified positions in the structure. It is found that the physical origin of the related phenomenon may be contributed by a combining effect of single-slit effect and interslits effect. The single-slit effect is brought by the excitation of surface-plasmon polaritons from the isolated slit and the interslits effect is caused by phase interference of the transmitted waves from two slits. When the transmissivity of an isolated slit is adjusted to a maximum, total transmissivity of the grating is never governed by phase interference and can be qualified to the contribution from a single slit alone.

DOI: 10.1103/PhysRevB.78.081404 PACS number(s): 42.79.Dj, 78.66.Bz, 42.25.Hz

The extraordinary optical transmission (EOT) of light through a thin metallic film perforated with periodic arrays of subwavelength holes or slits has received an ever increasing interest.[1–18] So far, for the EOT in slit structures, there are three influential mechanisms on its physical origin that appeared in the literatures. The first mechanism is the excitation of surface-plasmon polaritons (SPPs) at metal/dielectric interface.[3–5,9–11] The second explanation is based on dynamical diffraction theory.[12,13] The third mechanism is the transmission resonance of Fabry-Perot resonator formed by the slit with two ends open to free space.[4,14–16] In this theory, the exact origin of EOT is still debatable; for instance, Cao and Lalanne[14] have reported that the SPPs may play a negative role, thus leading to the suppression of the transmission. Therefore, the mechanisms on the EOT still are now under debate and discussion.[17] Recently, Schouten *et al.*[9] presented an experimental and theoretical study of EOT in a structure of two subwavelength width slits drilled on a thin metal screen. They observed oscillatory variation of transmission with the wavelength of the incident light beam. They suggested that the physical origin could be attributed to an interference effect, arising from the combination of the excitation of SPPs with their propagation along the surface from one slit to the other. This oscillation behavior was also observed in an experiment.[18]

Inspired by the works above, in this Rapid Communication, we present a time-domain analysis on the mechanism of plasmon-assisted Young's two-slit transmission. We employ the finite-difference time-domain (FDTD) algorithm[19] to study the variations of the energies with sampling time received by several monitors placed on the specified positions in structure. Our simulations clearly demonstrate that the involved physical origin is the combining effect of the excitation of SPPs from an isolated slit (referred as single-slit effect) and from an interference between the surface waves transmitted from two slits (referred as interslit effects).

We first prefer to revisit the Young's two-slit device studied by Schouten *et al.*[9] The structure is composed of two subwavelength width slits, separated by a distance of D, and drilled on a thin metal (silver) film with a thickness of 0.2 μm as sketched in the upper panel of Fig. 1. The structure is laid on the xy plane and the illumination light is normally launched upon the structure along the z axis. To analyze the physical mechanisms, we artificially settle three monitors of $M1$, planar $M2$, and $M3$ on the specified positions. Monitor $M1$ is put on the exit of the left slit (slit 1) and its receiving window faces to slit 1; therefore, only the energy passing through slit 1 is collected by $M1$. We have checked that the energy radiated from the exit surface of the structure is completely transmitted through the two slits rather than penetrating through metallic film; consequently, $M1$ receives half of the total energy. Planar monitor $M2$ is placed at a horizontal observation plane with a distance from the exit surface, with its receiving window facing to the exit surface of the structure. Its function is to receive the transmitted waves, which are passing through the two slits and further advancing to reach the far-field region. $M3$ is just

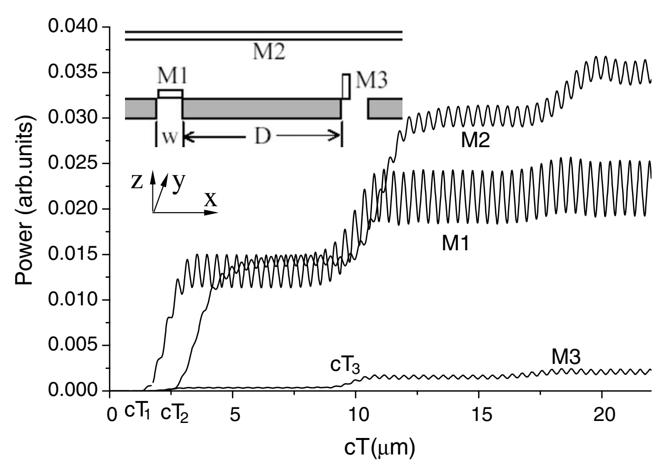

FIG. 1. Sketch of Young's two-slit experiment device on the upper panel and the variations of transmission energies collected by three monitors of M_1, M_2, and M_3 with the sampling time on the lower panel.

arranged on the left edge of the right slit (slit 2) and with a window facing left. Its function is to collect the energy of light, which transmits through slit 1 and then propagates along the upper surface (exit surface) of the film from slit 1 to slit 2. These monitors in the simulation software are set to be ideal and they do not influence the scattering field. In the simulations, we choose the following parameters: the dielectric constant of silver is evaluated by fitting the experimental data[20] where the fitting equation is $\epsilon=3.57-54.33\lambda^2+i(-0.083\lambda+0.921\lambda^3)$; thus, we obtain $\epsilon=-31.201+i0.405$ at the wavelength $\lambda=0.8$ μm; the width of each slit is $w=0.2$ μm and the distance from the right edge of slit 1 to the left edge of slit 2 is $D=8\lambda_{SPP}=8\times0.787=6.296$ μm, where λ_{SPP} is the SPP wavelength in the metal/air interface. The simulation domain is encircled by perfectly matched layer, which allows the light striking on the boundary to effectively leave the domain. The slab excitation with the width of 20 μm, which radiates a TM-polarized continuous wave (with the magnetic field parallel to the y axis) with the wavelength of $\lambda=0.8$ μm, is settled below the metallic film with a distance of 1 μm from the film.

The variations of the energy collected by three monitors of M_1, M_2, and M_3 with the sampling time cT are depicted by three curves marked with M_1, M_2, and M_3, respectively, in the lower panel of Fig. 1 where c is the light speed in vacuum. The onsets of these curves are denoted with cT_1, cT_2, and cT_3 respectively. We set $cT=0$ when light source begins to switch on. The light wave arrives at the exit of slit 1 (or slit 2) at the time of cT_1 and then the scattering wave from slit 1 (or slit 2) is divided into two parts and they travel along different channels: one part of the scattering waves from slit 1 is propagating along the exit surface of the thin film and then reaches slit 2, which is collected by monitor M_3 at the time of cT_3. We call it as the surface wave (or SPP wave). The second part of the scattering wave is propagating forward and is collected by monitor $M2$ (after a traveling time of cT_2-cT_1). It is clearly seen from Fig. 1 that the onset of curve $M1$ appears at cT_1 and then this curve reaches its first plateau, which manifests that the SPP-assisted resonance transmission in slit 1 is active now. Its second plateau stands up at cT_3, which implies that the surface wave generated at slit 2 has reached slit 1 and it leads to an increase in the transmission at slit 1. So the second plateau implies the interaction between the waves from the two slits (referred as interslits effect). It is known that the wave number of SPP in the metal (with dielectric constant ϵ_m)/dielectic (ϵ_d) flat interface is given by $k_{SPP}=\frac{\omega}{c}\sqrt{\frac{\epsilon_d\epsilon_m}{\epsilon_d+\epsilon_m}}=\frac{2\pi}{\lambda_{SPP}}$;[21] therefore, the wavelength of SPP on the free-standing silver film is $\lambda_{SPP}=0.787$ μm for the wavelength of light $\lambda=0.8$ μm. Consequently, the phase of the SPP wave transmitted from slit 2 to slit 1 and the phase of SPP excited by slit 1 is just in phase when the distance between two slits is chosen $D=8\lambda_{SPP}$ as addressed above. Thus, the interslits effect is attributed to the phase interference. Regarding curve $M2$, it exhibits similar profile with curve $M1$ except for a delay time of cT_2-cT_1, which is associated with the traveling time of light wave from the slit to the horizontal observation plane; consequently, curve $M2$ is moved—on the whole—rightward with respect to curve $M1$. These two plateaus in curve $M3$ stem from the same origin as that in curve $M1$. The function of $M3$ just serves as a measurement of the moment at which the surface wave arrives at slit 2, i.e., cT_3 or determines the interval of the travel of the surface wave from slit 1 along the film surface to slit 2, i.e., cT_3-cT_1.

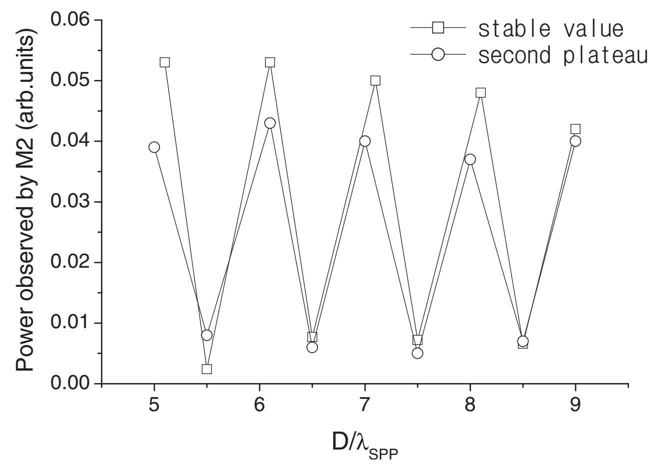

FIG. 2. Variations of transmission power collected by monitor $M2$ as a function of D. The circles (squares) represent the energy received by $M2$ at the second plateau (stable value) of curve, where the lines are drawn for guiding the eyes.

It is noticed that the third plateau at the moment about $cT=16$ μm is observed in each curve of Fig. 1. Its origin comes from the following mechanism: as we have mentioned above that the second plateau arises from the phase interference, for convenience, we refer it as the "first time interference". The enhanced power may excite the stronger SPP and then this SPP transmits from one slit to the other and leads to the stronger phase interference (referred as the "second time interference") and accordingly the stronger transmission; thus the third plateaus occur in Fig. 1. It is believed that for each curve, a series of plateaus should be successively formed after the third plateau, and they are contributed by what we call "multitime interference". Our calculations demonstrate that the series of plateaus tends to form a stable value rapidly when cT is increased, for instance, when cT is about 60 μm.

To reconfirm that the interslits effect is caused by phase interference, we provide another simulation with different D as shown in Fig. 2. The circles (squares) represent the energy received by $M2$ at the second plateau (stable value) of curve $M2$, where the lines are drawn for guiding the eyes. The curves exhibit periodic variation clearly. The energy transmission reaches its maximum (or minimum) when $D/\lambda_{SPP}=n$ (or $n+1/2$); n is integer.

There is an interesting question now: how about the influence on the EOT when the SPPs are simultaneously excited at both the lower and upper surfaces of the thin metal film? To answer this question, we prefer to consider a single-slit structure with slit width of $w=0.2$ μm and two silver slab walls are set up symmetrically at both sides of the slit as shown in Fig. 3(a). The right (left) silver slab wall is employed to reflect the waves from the slit that move rightward (leftward). A monitor is placed on the exit of the slit and the distance from the left (right) silver wall to the left (right)

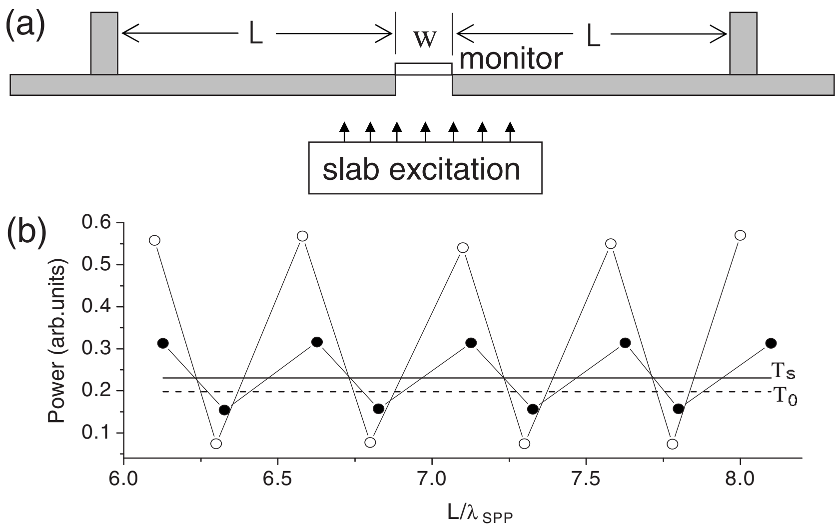

FIG. 3. (a) Schematic of a single slit milled on a thin metal film and two silver slab walls are set up symmetrically at either sides of the slit to reflect the rightward or leftward traveling light waves from the slit. A monitor is put on the exit edge of the slit and the distance from the left (right) silver wall to the left (right) edge of the slit is denoted with L. (b) Variations of the energy transmissions caused by the upper and lower SPPs as functions of L plotted by solid circles and open circles, respectively.

edge of the slit is denoted by L. The variations of the power corresponding to the second plateau as a function of L are displayed by solid circles in Fig. 3(b). The horizontal solid line (marked with T_s) represents the power measured by the monitor when both silver walls are removed, whereas the dashed line (denoted as T_0) represents the power received by the same monitor when the two walls and the two horizontal films are all removed. A perfect periodic oscillation around the horizontal solid line is observed in Fig. 3(b). All peaks (valleys) appear at about $2L/\lambda_{\mathrm{SPP}}=n$ $(n+1/2)$. These results can be well explained by the similar phase interference effect. Figure 3(b) indicates that phase interference may either enhance or suppress the transition, depending on the particular pattern or the phases of the waves that participate in the interference process, either in phase or out of phase.

The above phase interference comes from the SPP excited at the upper surface (upper SPP) exclusively because the two silver walls are placed on the upper surface. When placing the two walls on the lower surface, the SPP excited at the lower surface (lower SPP) will also result in the phase interference. The calculated results are shown with the open circles in Fig. 3(b). To compare with the solid circles, the curve of open circles exhibits oscillation with a larger amplitude; thus, it indicates that the phase interference from the lower SPP plays a more important role in the EOT. One striking feature of the curve of open circles, different from the curve of solid circles, is that the peak positions are much farther away from the horizontal solid line compared to the valleys. It means that the EOT enhancement caused by the lower SPP is stronger than the suppression due to the fact that the transmission should take a positive value and never be lower than zero, which is the lowest limitation. So in the case of the strong phase interference, the suppression of EOT does not match the enhancement of EOT; while the phase interference generated from the excitation of the upper SPP is not strong enough to reach the lowest limitation, as a result, the enhancement and the suppression of the EOT may be perfectly equal.

Figure 3(b) presents another interesting phenomenon: the transmission may still be enhanced significantly by a single-slit structure even without the interslits effect due to T_s (solid line) $>T_0$ (dashed line). To describe the single-slit effect, we define a relative transmissivity as $T_r=T_s/T_0$. The variation of T_r with the slit width w is displayed by the solid circles in Fig. 4. When $w>0.3$ μm, the results seem to follow the principle of geometric optics. However, when $w=0.1$ μm, a peak of $T_r=2.43$ appears; when $w=0.05$ μm, the transmissivity drops down rapidly. Figure 4 clearly demonstrates the mechanism of the EOT caused by an isolated slit referred as single-slit effect.

To further elaborate the single-slit effect, we investigate the Poynting vector distribution by setting the monitors on the slits with different slit widths and we observe the U-turn-like distribution in the slit region as sketched by the dashed curves in the insets on the top right corner of Fig. 4. In other words, the Poynting vector tends to be closer on the two walls of the slit. So we observe that the transmitted ability of the metallic surface is larger than that of the middle region (with air or without) of the slit. This phenomenon is referred as "surface effect". After comparing the plots in the two insets, it is found that the enhanced transmission energy is primarily contributed by an increase of the middle region of the slit when increasing the slit width. Consequently, the narrower the slit width, the higher the relative transmissivity

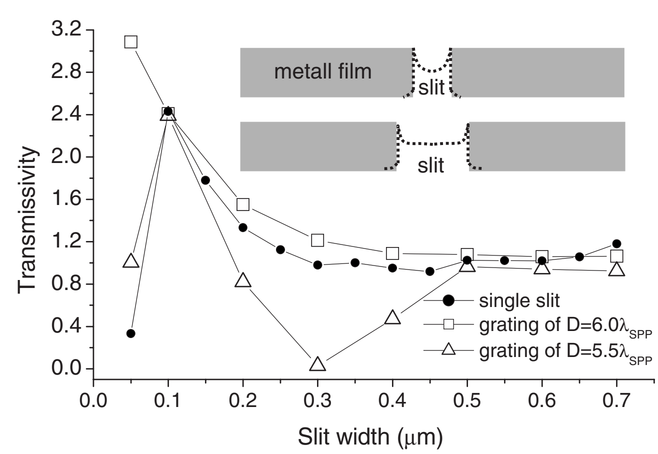

FIG. 4. Relative transmissivity in the single-slit structure and the silver grating structure for different slit widths.

is. On the other hand, the larger transmissivity of metallic surface is due to the contribution of SPP. As is well known, the SPP extends only over a thin layer in proximity to the metallic surface and decays rapidly in the normal direction of the metallic surface. When the SPP passes through a narrow slit, its extension scope will be limited; thus, this limitation will disturb the excitation of SPP on the metallic surface and decrease the transmissivity of the metallic surface referred as "antisurface effect". This corresponds to the case of $w=0.05$ μm. The surface and antisurface effects compete with each other in a slit and they will produce an optimal result corresponding to the case of $w=0.1$ μm. It should be noticed that the extended scope of the SPP on the metallic surface in a narrow slit is quite different from that on the flat surface. Since the real situation is rather complicated, therefore in this Rapid Communication, we offer a qualitative explanation only.

We have presented the two basic factors for the origin of the EOT: one is the single-slit effect and the other is interslits effect (phase interference). Now we study their combination in a metallic (silver) grating with subwavelength width slit and D, which is the distance between adjacent slits. The simulation results for $D=6$ and $5.5\lambda_{\mathrm{SPP}}$ are depicted by the open squares and triangles, respectively, in Fig. 4. It is apparent that when the slit width is larger than $w=0.1$ μm, especially in the range of about $w=0.2-0.4$ μm, the grating transmissivity depends on D. This result witnesses that the phase interference mechanism may play an important role in the metallic grating. When the slit width is increased continuously, for instance, the width of the slit exceeds $w=0.5$ μm, the phase interference becomes weaker gradually and T_r approaches the result of geometric optics. When the slit width is narrowed down, for instance, $w=0.05$ μm, both the square and triangle are located above the solid circle; so we know that, in both gratings of $D=5.5\lambda_{\mathrm{SPP}}$ and $D=6\lambda_{\mathrm{SPP}}$, only EOT enhancement may be observed without the suppression phenomenon. When $w=0.1$ μm, which corresponds to the case of the largest single-slit effect, the curves of both the squares and triangles become closer, almost overlapped. It means that the phase interference effect almost dies. Thus, it is concluded from Fig. 4 that when the single-slit effect reaches its maximum, for instance, $w=0.1$ μm, the phase interference effect becomes quite weak; as a consequence, the transmissivity of the grating approaches that of the single slit. The phase interference effect works actively in the case that the single-slit effect is unsaturated. However, the behavior of transmissivity in the range of $w\leq 0.1\mu m$ is unprecedented.

In summary, we investigate the EOT properties in the single-slit and the double-slit structures perforated on the thin silver film as well as the metallic (silver) grating. The interslits and single-slit effects are clearly analyzed in the time domain via the FDTD simulations. The single-slit effect reaches the largest for an optimal slit width, which is governed by the competition of surface and antisurface effects. The interslits effect is due to the phase interference generated from the excitations of the upper and lower SPPs; however, the lower SPP plays a more important role compared to the upper SPP. Both effects work together in the metallic grating. When the single-slit effect deviates from its maximum, the influence of phase interference on the transmission becomes considerable. In contrast, the phase interference effect becomes quite weak or unobservable. In this case, the transmissivity of silver grating approaches that of single slit. Our findings may deepen the understanding of the physical origin or mechanisms of the EOT.

This work was supported by the 973 Program of China (Grant No. 2006CB302901) and the Development Foundation of Beijing Education Commission in China (Grant No. KM200710028006).

*263zys@263.net
†guby@aphy.iphy.ac.cn

[1] T. W. Ebbesen, H. J. Lezec, H. F. Ghaemi, T. Thio, and P. A. Wolff, Nature (London) **391**, 667 (1998).
[2] H. F. Ghaemi, T. Thio, D. E. Grupp, T. W. Ebbesen, and H. J. Lezec, Phys. Rev. B **58**, 6779 (1998).
[3] U. Schröter and D. Heitmann, Phys. Rev. B **58**, 15419 (1998).
[4] J. A. Porto, F. J. Garcia-Vidal, and J. B. Pendry, Phys. Rev. Lett. **83**, 2845 (1999).
[5] P. Lalanne, J. P. Hugonin, and J. C. Rodier, J. Opt. Soc. Am. A **23**, 1608 (2006).
[6] D. E. Grupp, H. J. Lezec, T. W. Ebbesen, K. M. Pellerin, and T. Thio, Appl. Phys. Lett. **77**, 1569 (2000).
[7] L. Martin-Moreno, F. J. Garcia-Vidal, H. J. Lezec, K. M. Pellerin, T. Thio, J. B. Pendry, and T. W. Ebbesen, Phys. Rev. Lett. **86**, 1114 (2001).
[8] L. Salomon, F. Grillot, A. V. Zayats, and F. de Fornel, Phys. Rev. Lett. **86**, 1110 (2001).
[9] H. F. Schouten, N. Kuzmin, G. Dubois, T. D. Visser, G. Gbur, P. F. A. Alkemade, H. Blok, G. W. 't Hooft, D. Lenstra, and E. R. Eliel, Phys. Rev. Lett. **94**, 053901 (2005).
[10] P. Lalanne, J. P. Hugonin, and J. C. Rodier, Phys. Rev. Lett. **95**, 263902 (2005).
[11] A. Yu. Nikitin, F. Lopez-Tejeira, and L. Martin-Moreno, Phys. Rev. B **75**, 035129 (2007).
[12] M. M. J. Treacy, Appl. Phys. Lett. **75**, 606 (1999).
[13] M. M. J. Treacy, Phys. Rev. B **66**, 195105 (2002).
[14] Q. Cao and P. Lalanne, Phys. Rev. Lett. **88**, 057403 (2002).
[15] A. Barbara, P. Quemerais, E. Bustarret, T. Lopez-Rios, and T. Fournier, Eur. Phys. J. D **23**, 143 (2003).
[16] Alastair P. Hibbins, Matthew J. Lockyear, and J. Roy Sambles, J. Appl. Phys. **99**, 124903 (2006).
[17] T. D. Visser, Nat. Phys. **2**, 509 (2006).
[18] L. Aigouy, P. Lalanne, J. P. Hugonin, G. Julie, V. Mathet, and M. Mortier, Phys. Rev. Lett. **98**, 153902 (2007).
[19] K. S. Yee, IEEE Trans. Antennas Propag. **AP-14**, 302 (1966); in this letter, a commercially available software developed by Rsoft Design Group http://www.rsoftdesign.com is used for the numerical simulations.
[20] P. B. Johnson and R. W. Christy, Phys. Rev. B **6**, 4370 (1972).
[21] H. Raether, *Surface Plasmons on Smooth and Rough Surfaces and on Gratings* (Springer-Verlag, Berlin, 1988).